Reduction into a rational fraction of a thermodynamic property of the liquid state: Experimental determinations in the case of CO2 and nbutane. Extension to the other properties

Christiane Alba, Léon Ter Minassian, Armelle Denis, and Alain Soulard

Citation: The Journal of Chemical Physics **82**, 384 (1985); doi: 10.1063/1.448757
View online: http://dx.doi.org/10.1063/1.448757
View Table of Contents: http://scitation.aip.org/content/aip/journal/jcp/82/1?ver=pdfcov
Published by the AIP Publishing

Articles you may be interested in

A direct method of determining the coupling between internal molecular motions and transport properties: Application to liquid nbutane
J. Chem. Phys. **98**, 1524 (1993); 10.1063/1.464317

Statistical mechanics of small chain molecular liquids. II. Structure and thermodynamic properties of modeled nbutane liquid
J. Chem. Phys. **90**, 422 (1989); 10.1063/1.456491

Rational fraction representation of diatomic vibrational potentials. II. Application to H2 ground state
J. Chem. Phys. **73**, 5385 (1980); 10.1063/1.439929

Ideals gas thermodynamic properties and isomerization of nbutane and isobutane
J. Phys. Chem. Ref. Data **4**, 859 (1975); 10.1063/1.555526

An Empirical Equation for Thermodynamic Properties of Light Hydrocarbons and Their Mixtures I. Methane, Ethane, Propane and nButane
J. Chem. Phys. **8**, 334 (1940); 10.1063/1.1750658

This article is copyrighted as indicated in the article. Reuse of AIP content is subject to the terms at: http://scitation.aip.org/termsconditions. Downloaded to IP: 130.102.42.98 On: Mon, 24 Nov 2014 09:05:21

Reduction into a rational fraction of a thermodynamic property of the liquid state: Experimental determinations in the case of CO_2 and *n*-butane. Extension to the other properties

Christiane Alba and Léon Ter Minassian
Laboratoire de Chimie Physique, 11 Rue Pierre et Marie Curie, 75231 Paris Cedex 05, France

Armelle Denis
Laboratoire de Chimie Quantique (Université de Paris VI), Institut de Biologie Physico Chimique, 13 Rue Pierre et Marie Curie, Paris, France

Alain Soulard
Laboratoire de Minéralogie et de Cristallographie, Université Pierre et Marie Curie, 4 Place Jussieu, 75230 Paris Cedex 05, France

(Received 30 April 1984; accepted 16 July 1984)

The expansivity of liquid CO_2 and of *n*-butane is determined as a function of pressure up to 4 kbar, from the melting temperatures up to the critical temperatures. The experimental method is piezothermal. The set of data is processed through a fit with a multipoint Padé approximant using an algorithm due to Werner. This particular technique determines, in its reduced form, the unique rational function relevant to the problem. The expansivity of the whole liquid phase is described in terms of a simple equation with four coefficients which enables calculation of the other thermodynamic properties. The general aspect of the phenomenological equations is discussed in this instance, underlining the particular behavior of the heat capacity as a function of pressure.

Our knowledge of liquids is derived essentially from those equations of state which are suitable for the whole fluid phase. These equations are quite diverse, starting with the van der Waals' and becoming more and more elaborate as computational power increases along with experimental accuracy. The Benedict–Webb–Rubin, Altunin–Gadetskii, and other types of equations lead to remarkable results with respect to accuracy, but their algebraic representations are obtained only at the cost of an ever increasing number of coefficients which recently reached the figure of 74.[15,19] The main virtue of phenomenological equations is the simplicity which enables the immediate comprehension of their general behavior. This could prompt one to conclude that this quality of simplicity is lost.

The present work is consequently opposed to and confronts this conceptualization wherein such equations of state originate, i.e., it focuses on the description of the liquid state alone, extending the measurements in a pressure interval where the data are scarce. Our experimental method is based on the precise metrology of the expansivity α, as a function of pressure and temperature (p, T). To begin with, important experimental results had been overlooked for a long time in the computation of the equations of state.

Measuring the volume dependance with pressure at different temperatures, Bridgman[1,18] observed intersections of the isotherms of α. The interest of this phenomenon is related to the behavior of heat capacity C_p as a function of pressure, according to the following general equation:

$$(\partial C_p/\partial p)_T = -T(\partial^2 V/\partial T^2)_p = -VT[\alpha^2 + (\partial\alpha/\partial T)_p]. \quad (1)$$

The temperature derivative $(\partial\alpha/\partial T)_p$ is generally positive at low pressures. Following Bridgman, it becomes negative at higher pressures raising the question of the existence of a minimum of C_p as a function of pressure. This important detail was only recently incorporated with a new equation of state.[20] The other interesting aspect of liquid phase thermodynamics has a more theoretical character. It concerns the properties of the phase in the metastable region especially in the vicinity of the line of instability spinodal predicted by the van der Waals equation. Defined as the locus of the divergence of the compressibility κ this line is located in the (p, T) plane mainly by means of extrapolation from the stable liquid phase. This aspect requires a careful choice of the phenomenological equations which should agree with the thermodynamic relationships when approaching the limits of the metastable phase.

Our metrology is the piezothermal one, which has been fully described over the last ten years.[2–4] However, in the present case, a new type of calorimeter has been used, based on a pneumatic principle. The main features of this calorimeter were given in the specialized literature,[5] however, a survey of its working principles will be given here. Finally an objective processing of the experimental data was performed through a rational interpolation (*N*-Padé approximants). A specific algorithm due to Werner[6] was chosen because of its stability and generality. The use of this algorithm and its particular interest compared to the least squares method will also be stressed in the present work.

I. APPARATUS AND METHOD

The piezothermal method determines the expansivity α by measuring the heat of compression. Under isothermal conditions the thermodynamic equations of Maxwell may be written in the following form:

$$\delta q' = TdS/V = -\alpha T dp, \quad (2)$$

where $\delta q'$ is the quantity of heat released from a unit volume

 0021-9606/85/010384-10$02.10 © 1985 American Institute of Physics

This article is copyrighted as indicated in the article. Reuse of AIP content is subject to the terms at: http://scitation.aip.org/termsconditions. Downloaded to IP: 130.102.42.98 On: Mon, 24 Nov 2014 09:05:21

of a sample undergoing a variation of the pressure. For a sample which is observed to release a quantity of heat δq from a constant volume v_e, we have

$$\delta q = v_e \delta q' = -\alpha v_e T dp. \quad (3)$$

The final result is obtained by integrating over a not too large pressure interval Δp in order to neglect the variation of α within this interval. The final result may be written in the following form:

$$(\alpha - \alpha_r) = -q/v_e T \Delta p, \quad (4)$$

where α_r is a corrective term arising from the contribution of the vessel to the overall thermal effect. It may be identified with the expansivity of the vessel material for the simple case of a continuous infinite tube.

The quantity of heat is measured by two types of calorimeters chosen according to their working temperatures. The first is a flux calorimeter working in the (+ 30, + 200 °C) temperature range and its use with a piezothermal device has been described elsewhere.[7] The second calorimeter is based on a pneumatic principle and has been developed in our laboratory. Its working temperature is the range between − 200 and + 80 °C. It is, as a matter of fact, a compensation calorimeter opposing a known quantity of heat Q_c to the quantity Q released from a sample such that $Q_c = Q$. This is obtained by varying the pressure P of an ideal gas contained in a bulb with an internal volume v_b in order to keep the temperature constant. As for an ideal gas $\alpha = 1/T$, Eq. (3) may be simply written as

$$Q_c = Q = -v_b \Delta p. \quad (5)$$

Equation (5) establishes a proportional relation between a quantity of heat and a pressure. This fact opens the way for a new type of calorimeter which converts the measurement of a quantity of heat into a more easily performed pressure measurement. The pneumatic calorimeter is schematically shown in Fig. 1, full details are given in the literature.[5]

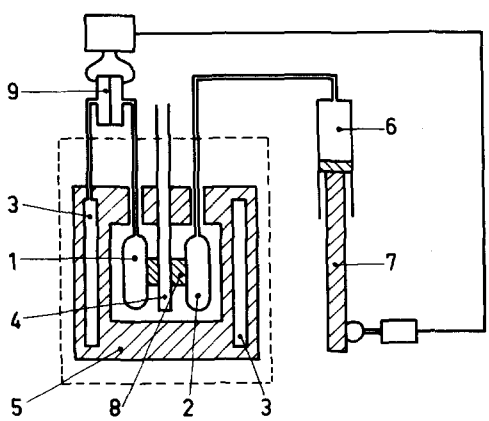

FIG. 1. The pneumatic calorimeter. Sample—positioned in the access tube 4. It is an autoclave of 1.7 cm outer diameter and 8 cm height. Internal volume $v_e = 1.213$ cm^3. Temperature detection—thermometric bulbs 1 and 3 are connected to a differential membrane manometer gauge 9. It is a constant volume gas thermometer detecting temperature differences down to 0.1 microdegrees. Reference temperature is given by thermal capacity 5. Heat compensation—bulb 2 containing helium gas under a pressure of a few bars. The pressure adjustment is performed with the pump cylinder 6 and piston 7 moved by an electrical screw jack. Operating conditions—bulbs and sample are in thermal connection by means of copper braces 8. The signal from the manometer is fed to the pump system in order to set the temperature difference back to zero.

The high pressure part of the piezothermal device is composed of a high pressure autoclave with a Bridgmann closure on one end, while the other end is connected to a pressure multiplier by means of a high pressure tube. Pressures as high as 7 kbar can be established in the system. These are measured by two conventional pressure gauges—a Manganin pressure gauge supplied from Harwood for the 200–7000 bar pressure range and a strain gauge from Sedeme for the 1–200 bar range. The resolution of the gauges are ± 1 and $\pm 5.10^{-2}$ bar, respectively. The experimental procedure is the same for both calorimeters. Their temperatures being adjusted to their working values and the autoclaves being positioned at the bottom of their access tubes, the highest pressure is established in the high pressure circuit. The system is allowed to rest for a few hours to reach thermal equilibrium then by small steps of about 10 or 100 bar, the pressure is decreased down to the saturation pressure. At each step, the quantity of heat is measured and the expansivity α determined from Eq. (4). A typical curve is given in Fig. 2.

II. THE PROCESSING OF THE DATA

The fit of the experimental points with an arbitrary function is usually performed by the least squares method. This method gives all the desired accuracy provided the number of coefficients be sufficient. In general, the experimenter stops when the accuracy of the fit is of the same order of magnitude as the experimental one. In no way does this method give one a means to discern if, for instance, a given set of points belongs to a quadratic, cubic, or other order polynomial, if the chosen arbitrary function had been a polynomial.

Our purpose is to identify the analytical form of a given function. The choice of a suitable method relevant to this problem of detection of form, is also inspired by the main features of the experimental curves:

(i) Some curves have singularities at low pressures depending on the temperature;

(ii) The experimental points are but slightly scattered;

(iii) An analytical representation with a rational fraction is *a priori* realistic.

The foregoing features led us to choose the rational interpolation method known as multipoint Padé approximant. A multipoint Padé approximant is a rational fraction $[L/M] = P^L(z)/Q^M(z)$, where $P^L(z)$ and $Q^M(z)$ are polynomials of the L th and M th order, respectively, which reproduces the values of a given function through different points.[8] The choice of an algorithm suited for the construction of the Padé approximant is of great importance as regards the stability of the results. More precisely, the experimental data being necessarily of limited accuracy, a slight change in the initial data should also induce a small change in the final results of the Padé approximant computation. For this purpose, we used the algorithm recently developed by Werner[6] based on the generalized continuous fractions of Thiele. This algorithm allows one to simultaneously explore all the experimental points and also to systematically reduce their number in order to get the rational fraction of the required degree. Before going any further the following point

This article is copyrighted as indicated in the article. Reuse of AIP content is subject to the terms at: http://scitation.aip.org/termsconditions. Downloaded to IP: 130.102.42.98 On: Mon, 24 Nov 2014 09:05:21

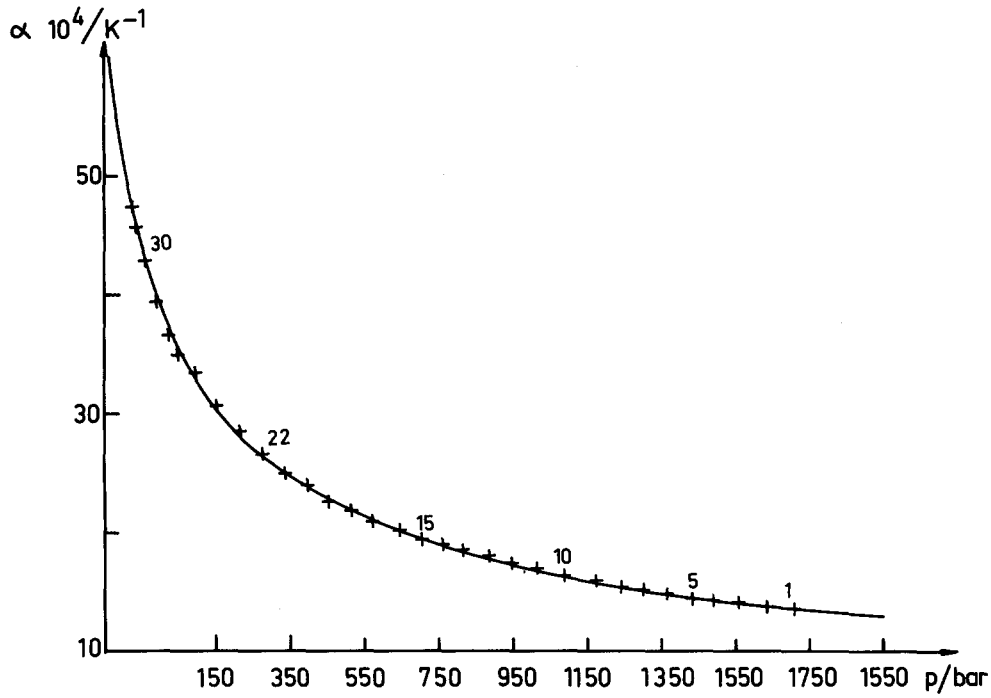

FIG. 2. A typical experimental curve. The 253.1 K isotherm in the case of CO_2 (32 experimental points). The full curve is computed wth Eq. (7) determined by the points numbered 30 and 22.

has to be emphasized: In general it is always possible to interpolate a given experimental function by a rational function. However, if from physical considerations one knows *a priori* that the analytical expression of an experimental function is a rational function $P^l(z)/Q^m(z)$, then the Padé approximant $P^L(z)/Q^M(z)$, where $L \geqslant l$ and $M \geqslant m$ will be reduced to the approximant $P^l(z)/Q^m(z)$.

This reduction is easily visualized when the approximant P^L/Q^M is written as a function of the roots $\{\tau_i\}$ and $\{\beta_j\}$ of the polynomials of the numerator and the denominator, respectively,

$$[L/M] = \frac{P^L(z)}{Q^M(z)} = \frac{a_L}{b_M} \frac{\prod_{i=1}^{L}(z-\tau_i)}{\prod_{j=1}^{M}(z-\beta_j)}, \tag{6}$$

where a_L and b_M are the coefficients of highest power in z of P^L and Q^M polynomials, respectively.

As the approximant P^L/Q^M reduces to the approximant P^l/Q^m, this means that two sets of roots $\{\tau_k\}$ and $\{\beta_k\}$ $(k = m+1, m+2, \ldots, M)$ are mutually balanced. Consequently if the analytical expression of an experimental curve is a rational function of a given order and if one begins with a rational fraction of a higher order, this reduction will occur by the foregoing mechanism.[9,10] The construction of the Padé approximant $[L/M]$ requires $(L+M+1)$ experimental points. Within the framework of the Werner algorithm, it is always possible to start with the polynomials of the highest order by processing the whole set of experimental points and to gradually reduce their number after inspection of the roots occurring in the numerator and the denominator of Eq. (6).

The processing of our experimental points relies on these principles using the following three-step procedure:

(i) Each isotherm is separately processed in search of an analytical function $\alpha = f(p)$ in the form of Eq. (6). As the set of data of an isotherm points to the existence of a divergence for a particular pressure value p_λ, the approximant (6) would lead to a logarithmic singularity when computing the integral of α. This difficulty is avoided by setting $\alpha^n = F(p)$, where $n > 1$ insures the convergence of the integral of α.

A selection of experimental points (α_k, p_k) is prepared in the form of a set of pairs (α_k^n, p_k). This set is first examined for large values of p_k in order to determine the difference $(L-M)$ in Eq. (6). Then, introducing this set as initial data into the Werner program, the result is examined for the presence of inaccessible points linked to the existence of large experimental errors. In this instance, the point selection is changed in order to obtain a regular curve resulting from the approximant $F(p)$, then the value of n giving the maximum reduction of the approximant is chosen which leads to the following result with $M = 1$, $L = 0$, $n = 2$, i.e.:

$$\alpha^2 = \gamma_1/(1+\gamma_2 p). \tag{7}$$

Two selected points are enough for the interpolation of the whole set of experimental data. This selection is changed in order to obtain the minimum quadratic error. This determines the final values of the constants γ_1 and γ_2. The curve given in Fig. 2 shows the resulting fit with a relative error of 0.86%. A specific example of how the choice of n, M, and L has been made is given in the Appendix.

(ii) The coefficients in Eq. (7) vary with the temperature. Setting $A^2 = \gamma_1/\gamma_2$ and $p_\lambda = -1/\gamma_2$, Eq. (7) may be written as follows:

$$\alpha = A/(p-p_\lambda)^{1/2}. \tag{8}$$

Equation (8) brings out the role of p_λ which defines the locus of the divergence of α in the (p, T) plane. The corresponding approximant is computed as a function of temperature from a suitable selection of experimental points including the coordinate point $(p = p_c, T = T_c)$, so that the locus $p_\lambda(T)$ passes through the critical point. The result is a rational function $(L = 1, M = 1)$:

This article is copyrighted as indicated in the article. Reuse of AIP content is subject to the terms at: http://scitation.aip.org/termsconditions. Downloaded to IP: 130.102.42.98 On: Mon, 24 Nov 2014 09:05:21

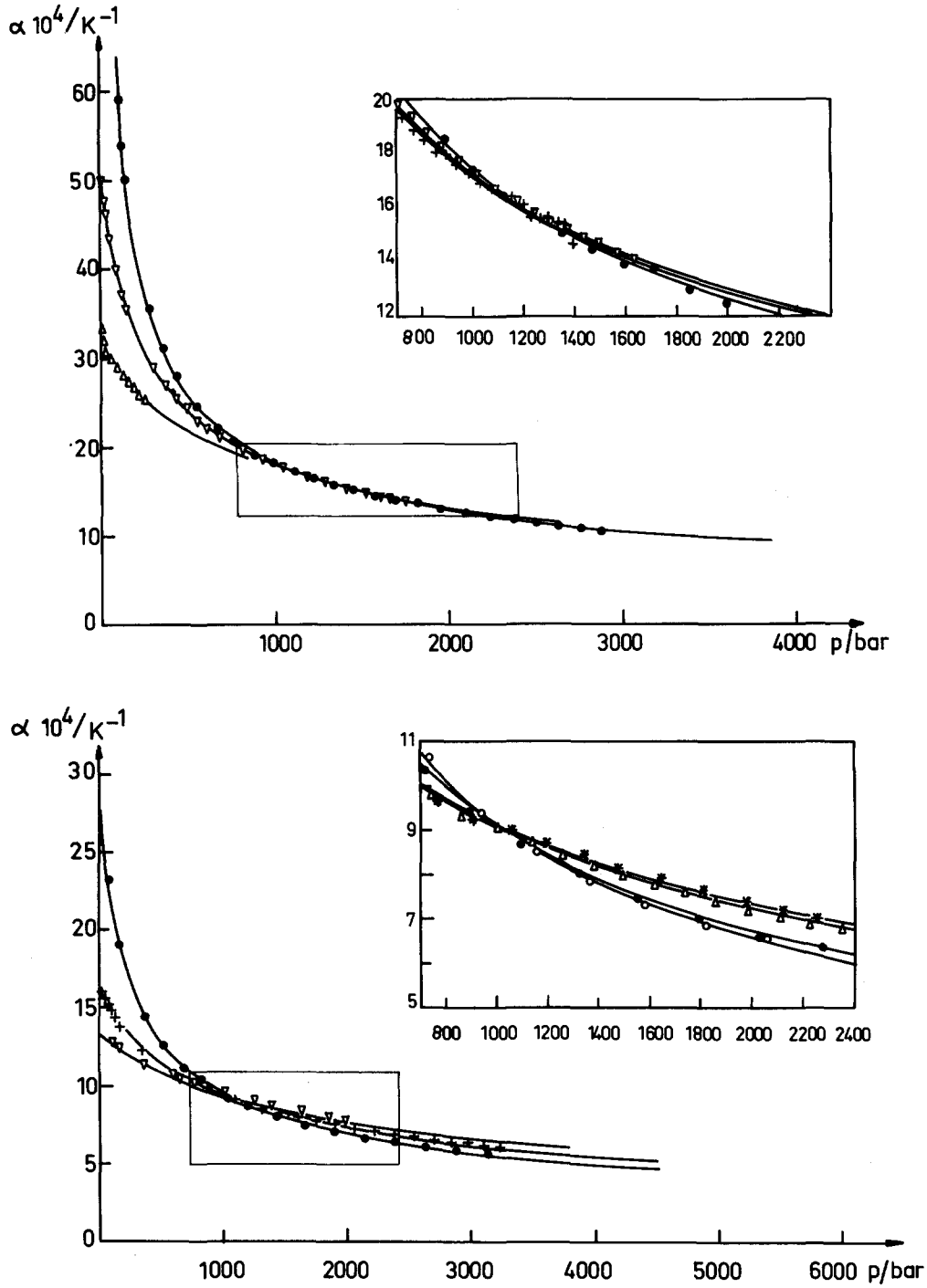

FIG. 3. A survey of the final fit with the experimental points. Full curves are computed from Eq. (10). Insights show the intersection of the isotherms through a single point. (a) Isotherms of carbon dioxide: △221.5 K, + 243.7 K, ▽253.1 K, ●284.7 K; (b) Isotherms of *n*-butane: ▽181.4 K, ∗204.9 K, △228.5 K, + 243.9 K, ●345.3 K, ○410.8 K.

TABLE I. The four constants of Eqs. (9) and (10), determined from a final least squares fit with the whole set of data. Accuracy is about 1.5%. The number of experimental points is 211 (7 isotherms) and 266(11 isotherms) in the case of CO_2 and *n*-butane, respectively. Critical constants—V_c, p_c, and T_c.

	V_c/cm³ mol⁻¹	p_c/bar	T_c/K	a_1	a_2	p_0/bar	α_0/K⁻¹
CO_2	94.429	73.83	304.21	− 13.8704	− 1.98327	1250	16.330×10^{-4}
n-Butane	255.102	37.97	425.16	− 19.4579	− 1.06454	1100	9.109×10^{-4}

This article is copyrighted as indicated in the article. Reuse of AIP content is subject to the terms at: http://scitation.aip.org/termsconditions. Downloaded to IP: 130.102.42.98 On: Mon, 24 Nov 2014 09:05:21

$$m_\lambda = (a_1 t + 1)/(a_2 t + 1), \tag{9}$$

where m_λ and t are the reduced pressures and temperatures

$$m_\lambda = p_\lambda/p_c, \quad t = (T_c - T)/T_c. \tag{9a}$$

(iii) The foregoing results should be refined in order to take into account the intersections of the isotherms of α as may be seen in Figs. 3(a) and 3(b). The coefficient A in Eq. (8) is rather insensitive to the variation of the temperature and is no help in defining the locus of the intersections. However, inspection of the insets [Figs. 3(a) and 3(b)] shows that they occur in a very small region pointing to the existence of a single intersection point of coordinate $(\alpha_0, p_0 = m_0 p_c)$. Equation (8) is modified accordingly and gives with $m = p/p_c$:

$$\alpha(m, t) = \alpha_0 \left[\frac{m_0 - m_\lambda}{m - m_\lambda}\right]^{1/2}. \tag{10}$$

The set of four constants α_0, m_0, a_1, and a_2 in Eqs. (9) and (10) determines the expansivity through the whole liquid phase excepting the vicinity of the critical region. Their values resulting from a final fit by the least square method are given in Table I for CO_2 and *n*-butane. The resulting curves computed from Eqs. (9) and (10) are also given in Figs. 3(a) and 3(b) and show the quality of the fit with our experimental data. Figure 4 allows a comparison with the data given in the literature.

III. THE OTHER THERMODYNAMIC FUNCTIONS

The expansivity determines the volume and the compressibility (V, κ), as a function of the variables (p, T) following the general equations:

$$\ln V = \int \alpha \, dT, \tag{11a}$$

$$\kappa = -\int (\partial\alpha/\partial p)_T \, dT. \tag{11b}$$

Equations (11a) and (11b) may be integrated algebraically. Beginning with the volume, substitution of $T = g(m_\lambda)$ from Eq. (9) and α from Eq. (10) allows one to set Eq. (11a) out in the following form:

$$\ln V = \Omega \int \left(\frac{m_0 - m_\lambda}{m - m_\lambda}\right)^{1/2} \cdot \frac{dm_\lambda}{(m_\lambda - \omega)^2} \tag{12}$$

with

$$\Omega = \frac{(1 - \omega)\alpha_0 T_c}{a_2}, \quad \omega = a_1/a_2. \tag{12a}$$

Performing the change of variable $X^2 = (m_0 - m_\lambda)/(\omega - m_\lambda)$ reduces Eq. (12) into one of the forms given in the literature.[21] The result is

$$\ln \frac{V(m, m_\lambda)}{V(m, m_{\lambda r})} = \frac{\Omega}{(m - \omega)} \left[\frac{(m_0 - m_\lambda)^{1/2}(m - m_\lambda)^{1/2}}{(\omega - m_\lambda)} - \frac{m_0 - m}{(m_0 - \omega)^{1/2}} \mathcal{J}\right]_{m_{\lambda r}}^{m_\lambda}, \tag{13}$$

where the integral has been performed between the temperature T and a reference temperature T_r, which accordingly determines the limits m_λ and $m_{\lambda r}$ [Eq. (9)]. The function $\mathcal{J}$ takes one of the following two forms depending on the value of m: for $m < \omega$,

$$\mathcal{J} = \frac{1}{(\omega - m)^{1/2}} \arcsin \left\{\frac{(m_0 - m_\lambda)(\omega - m)}{(m_0 - m)(\omega - m_\lambda)}\right\}^{1/2}; \tag{13a}$$

for $m > \omega$,

$$\mathcal{J} = \frac{1}{(m - \omega)^{1/2}} \ln \frac{\sqrt{(m_0 - m_\lambda)(m - \omega)} + \sqrt{(m - m_\lambda)(m_0 - \omega)}}{\sqrt{(\omega - m_\lambda)}}; \tag{13b}$$

for $m = \omega$, the result is

$$\ln \frac{V(m = \omega, m_\lambda)}{V(m = \omega, m_{\lambda r})} = \frac{2}{3} \frac{\Omega}{(m_0 - \omega)} \left[\left(\frac{m_0 - m_\lambda}{\omega - m_\lambda}\right)^{3/2}\right]_{m_{\lambda r}}^{m_\lambda}. \tag{13c}$$

The same substitutions allow the integration of Eq. (11b). The result for the compressibility is

$$\kappa(m, m_\lambda) - \kappa(m, m_{\lambda r}) = \frac{\Omega}{(m - \omega)^2 p_c} \left[\frac{(m_0 - m_\lambda)^{1/2}}{(m - m_\lambda)^{1/2}} + \frac{(m_0 - m_\lambda)^{1/2}(m - m_\lambda)^{1/2}}{2(\omega - m_\lambda)} - \frac{(m_0 - m) + 2(m_0 - \omega)}{2(m_0 - \omega)^{1/2}} \mathcal{J}\right]_{m_{\lambda r}}^{m_\lambda}, \tag{14}$$

where the function $\mathcal{J}$ takes the form of either Eq. (13a) or Eq. (13b) depending on the sign of $(m - \omega)$.

For $m = \omega$, the result is:

$$\kappa(m = \omega, m_\lambda) - \kappa(m = \omega, m_{\lambda r}) = \frac{\Omega}{(m_0 - \omega)^2 p_c} \left[\frac{1}{5}\left[\frac{m_0 - m_\lambda}{\omega - m_\lambda}\right]^{5/2} - \frac{1}{3}\left[\frac{m_0 - m_\lambda}{\omega - m_\lambda}\right]^{3/2}\right]_{m_{\lambda r}}^{m_\lambda}. \tag{14a}$$

This article is copyrighted as indicated in the article. Reuse of AIP content is subject to the terms at: http://scitation.aip.org/termsconditions. Downloaded to IP: 130.102.42.98 On: Mon, 24 Nov 2014 09:05:21

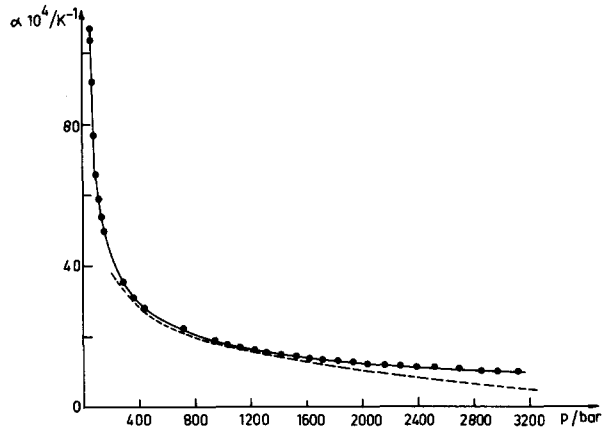

FIG. 4. A comparison in the case of CO_2 with the equation of state of Altunin-Gadetskii (Ref. 15). The 273.6 K isotherm---computed from the equation. ● our results.

Finally the heat capacity follows from the integration of Eq. (1) as a function of pressure. As no simple algebraic expression could be calculated, the numerical integration is done resulting in the tabulation of the quantity (Tables III and IV)

$$C_p(p_r, T) - C_p(p, T), \tag{15}$$

where p_r is a reference pressure.

IV. THE REFERENCE CURVES

The knowledge of two reference curves determines the absolute quantities V, κ, and C_p. The reference curves are an isotherm for the volume $V(T_r)$ and an isobar for the heat capacity $C_p(p_r)$ which may be constructed from the data found in the literature. This is achieved by the Werner algorithm which defines the degree of the rational fraction appropriate to the case and the result is refined by the least squares method. The source of the data and the results of the fit are given in the following.

A. Reference isotherms for the volume $V(T_r) = f(p)$

The high pressure and low temperature data for CO_2 are very sparse. The volumetric data at $T > T_c$ and high pressures are extrapolated in order to bring them to the 300 K isotherm.[13] This procedure links a set of high pressure data to the one given in the I.U.P.A.C. tables below 1 kbar.[11] An appropriate fit for both sets is obtained with a rational fraction determining the algebraic expression of the 300 K isotherm. The extrapolation of this isotherm in the direction of the low pressures side cannot be carried very far because of an overly high temperature which places the singularity of V at $p_\lambda > 0$. To keep the possibility of examining the properties on the negative pressure side, the 300 K isotherm is taken as a reference for the computation of a 220 K isotherm using the appropriate Eq. (13). This procedure does not introduce any additional error and the 220 K isotherm, represented with a rational function [1/1] is taken as a reference for CO_2. In the case of *n*-butane, accurate data are those of the N.B.S. up to 700 bar.[12] An analysis by Jorgensen[14] extrapolates the

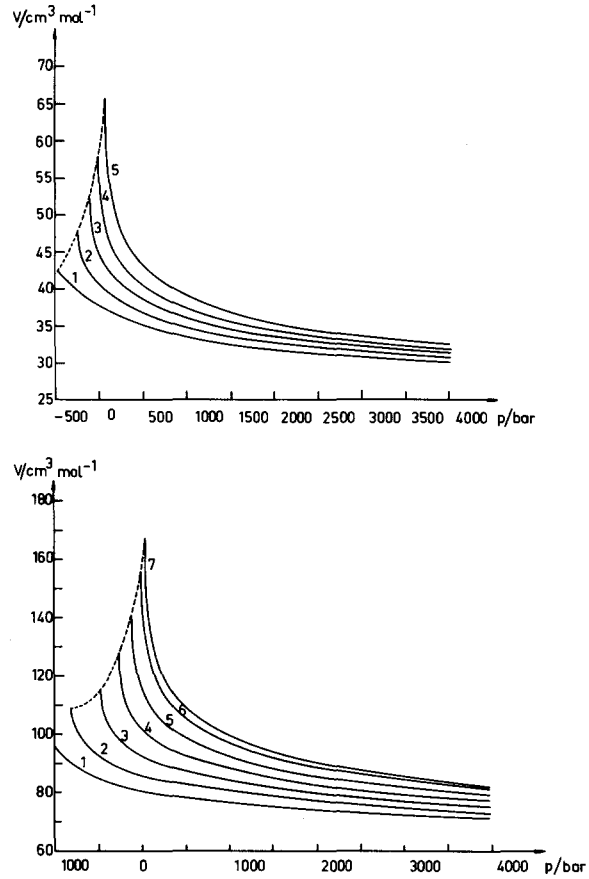

FIG. 5. The molar volumes.---locus V_λ as a function of pressure. (a) Carbon dioxide. Isotherms 1–5: 220, 240 K,... and T_c, respectively. (b) *n*-butane. Isotherms 1–7: 150, 250 K,... and T_c, respectively.

TABLE II. The constants for the reference volumes and heat capacities according to Eqs. (16) and (17), respectively. They agree with the pressure in bars and temperature in K. Reference isotherms and isobars: T_r and p_r, respectively.

(A)	T_r/K	f_1	f_2	g_0	g_1	g_2		
CO_2 V/cm³mol⁻¹	220	4.6450×10^{-4}	0.0000	2.6470×10^{-2}	1.7123×10^{-5}	0.0000		
n-Butane V/cm³ mol⁻¹	150	6.1508×10^{-4}	1.3908×10^{-8}	1.2400×10^{-2}	8.5678×10^{-6}	3.2676×10^{-10}		
(B)	p_r/bar	u_1	u_2	u_3	v_0	v_1	v_2	v_3
CO_2 C_p/J K⁻¹ mol⁻¹	500	-8.4212×10^{-3}	1.8232×10^{-5}	0.0000	1.4362×10^{-2}	-1.1895×10^{-4}	2.5336×10^{-7}	0.0000
n-Butane C_p/J K⁻¹ mol⁻¹	700	-6.5977×10^{-3}	2.7151×10^{-5}	-3.9714×10^{-8}	6.0979×10^{-3}	-2.0264×10^{-5}	7.1888×10^{-8}	-1.3110×10^{-10}

This article is copyrighted as indicated in the article. Reuse of AIP content is subject to the terms at: http://scitation.aip.org/termsconditions. Downloaded to IP: 130.102.42.98 On: Mon, 24 Nov 2014 09:05:21

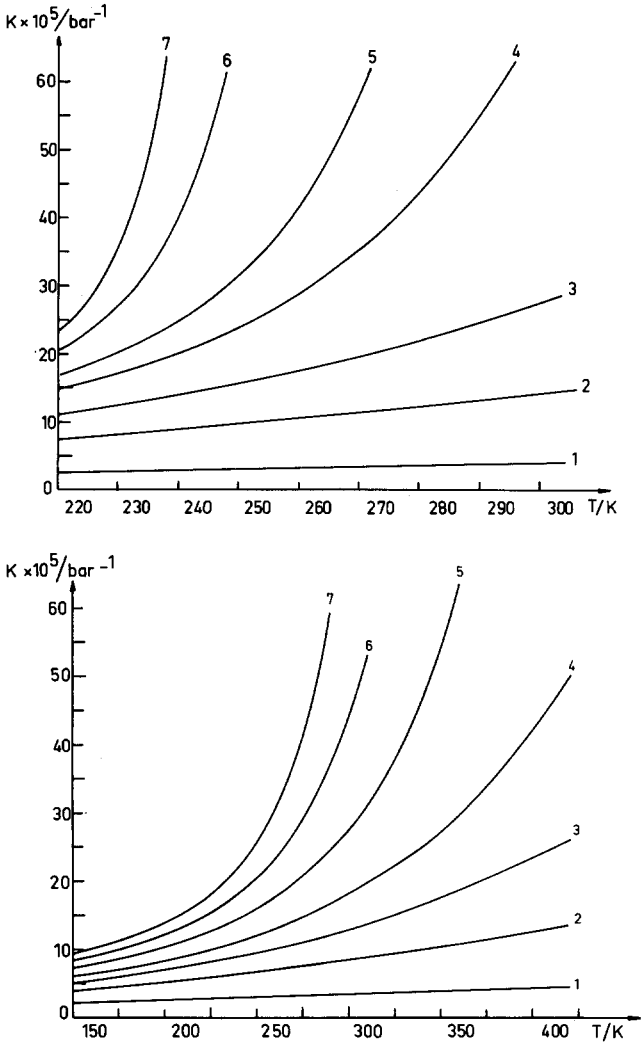

FIG. 6. The compressibility as a function of temperature. (a) Carbon dioxide. Isobars 1–7: 3000, 1000, 500, 200, p_c, −100, −200 (in bar units), respectively. (b) *n*-butane. Isobars 1–7: 3000, 1000, 500, 250, p_c, −100, −200 (in bar units), respectively.

data for higher hydrocarbon chains down to the case of *n*-butane and determines the relative volumes from 1 to 15 000 bar. This collection of data is processed—using Eq. (13)—in order to compute the 150 K isotherm which fits a rational function [2/2]. The values of the coefficients which appear in the following equation are given in part (A) of Table II:

$$V(T_r)=\frac{1+f_1p+f_2p^2}{g_0+g_1p+g_2p^2}. \tag{16}$$

A survey of the absolute quantities V and κ are given in Figs. 5(a) and 5 (b) and Figs. 6(a) and 6(b) for CO_2 and *n*-butane, respectively.

B. Reference isobar for the heat capacity $C_p(p_r) = f(T)$

The complete data source for CO_2 and *n*-butane is found in the I.U.P.A.C. and N.B.S. tables, respectively. Both were fitted with rational fractions of the following form:

$$C_p(p_r)=\frac{1+u_1T+u_2T^2+u_3T^3}{v_0+v_1T+v_2T^2+v_3T^3}. \tag{17}$$

The coefficients in Eq. (17) are given in Part (B) of Table II, and Figs. 7(a) and 7(b), give the general aspect of the behavior of the absolute heat capacity as a function of pressure.

V. RESULTS AND DISCUSSION

The expansivity α and also the variations $V/V_r, \Delta\kappa$ are determined by the straightforward computation of Eqs. (10), (13), and (14), respectively, with the four coefficients given in Table I. The variation of ΔC_p is obtained by the numerical integration of Eq. (1) along an isotherm under the same conditions. In spite of the fact that this last computation requires information for a reference volume, this limitation does not introduce any additional significant error. Therefore, the quantities α, V/V_r, $\Delta\kappa$, and ΔC_p may be considered as the self-consistent set of thermodynamic properties resulting solely from the piezothermal method. The "exactness" of these functions in relation to the properties they describe, may be characterized by three criteria—simplicity, accuracy, and conformity with the laws of thermodynamics. Setting the first two criteria simplicity of four coefficients and 1.5% accuracy aside, the problem is to examine the behavior of the functions in the vicinity of the limits where they diverge or become singular.

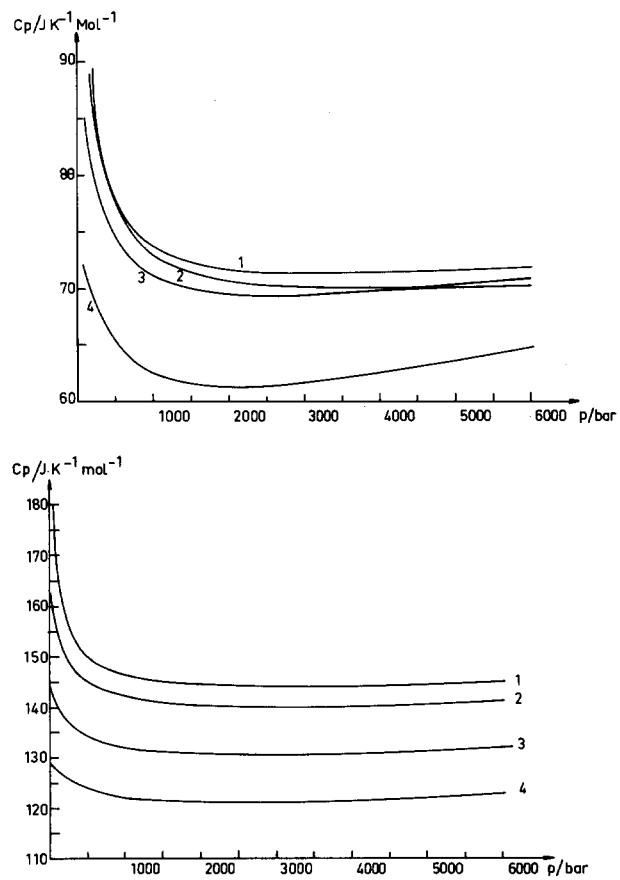

FIG. 7. The heat capacity as a function of pressure. (a) Carbon dioxide. Isotherms 4–1: 220, 250, 280, 300 K, respectively. (b) *n*-butane. Isotherms 4–1: 250, 300, 350, 400 K, respectively.

This article is copyrighted as indicated in the article. Reuse of AIP content is subject to the terms at: http://scitation.aip.org/termsconditions. Downloaded to IP: 130.102.42.98 On: Mon, 24 Nov 2014 09:05:21

TABLE III. *n*-Butane—difference of heat capacity ΔC_p/J K^{-1} mol^{-1} from pressure p to pressure $p = 50$ bar.

	T/K						
p/bar	150	200	250	300	350	400	420
6000	0.17	2.41	5.34	9.53	16.64	35.37	65.23
5000	1.08	3.17	5.98	10.05	17.07	35.71	65.53
4000	1.92	3.88	6.57	10.53	17.43	35.97	65.76
3000	2.61	4.46	7.02	10.86	17.65	36.08	65.82
2000	2.98	4.72	7.15	10.85	17.50	35.77	65.45
1000	2.56	4.07	6.25	9.67	16.01	33.96	63.50
900	2.44	3.89	6.02	9.39	15.66	33.53	62.95
800	2.29	3.69	5.74	9.04	15.22	33.01	62.32
700	2.12	3.44	5.41	8.61	14.69	32.34	61.56
600	1.91	3.14	5.00	8.08	14.01	31.49	60.59
500	1.67	2.79	4.51	7.41	13.12	30.35	59.31
400	1.40	2.36	3.89	6.55	11.94	28.75	57.49
300	1.07	1.85	3.12	5.41	10.29	26.33	54.66
200	0.69	1.22	2.13	3.85	7.80	22.18	49.47
100	0.25	0.45	0.82	1.58	3.56	12.77	35.04
50	0	0	0	0	0	0	0

A. Analytical behavior approaching the limit $m \to m_\lambda$

The conformity with the limiting laws can be checked when the pressure $p_\lambda = m_\lambda p_c$ in the plane (p, T) is identified with the pseudocritical line in the sense of Compagner.[16] This line is the locus of the divergence of the quantities α, κ, and C_p which were shown to match with equal pseudocritical exponents. According to the predictions of the classical theory, the isobaric or the isothermal approach to the limiting line should be characterized by divergencies of the form $(T_\lambda - T)^{-1/2}$ and $(p - p_\lambda)^{-1/2}$ for all the derived quantities.[17]

In view of the behavior of our phenomenological equations and beginning with α[Eq. (10)] the isothermal approach is naturally of the form $(m - m_\lambda)^{-1/2}$. The approach along the m_1 isobar defines the temperature t_λ of the divergence according to Eq. (10a). The limiting form of α when $t \to t_\lambda$ then is found to be

$$\alpha = \frac{\alpha_0 t^{3/2}}{(1 - m_1)}(m_0 - m_1)^{1/2}(a_2 - a_1)^{1/2}(t - t_\lambda)^{-1/2}, \quad (18)$$

i.e., $\alpha \sim (T_\lambda - T)^{-1/2}$.

Examination of the compressibility behavior [Eq. (14)] when $m \to m_\lambda$ immediately gives:

$$\Delta\kappa = \frac{\Omega}{(m_\lambda - \omega)^2 p_c}\frac{\alpha}{\alpha_0} \sim \kappa \sim \alpha. \quad (19)$$

Equation (19) establishes a proportional relation with the expansivity. The same is true for the heat capacity given by the general equation (1) and Eq. (10). Neglecting the variation of the volume and retaining the dominant term when $\alpha \to \infty$, the integration of Eq. (1) gives

TABLE IV. CO_2—difference of heat capacity ΔC_p/J K^{-1} mol^{-1} from pressure p to pressure $p = 100$ bar.

	T/K								
p/bar	220	230	240	250	260	270	280	290	300
6000	6.77	8.90	11.11	13.53	16.34	19.81	24.45	31.41	44.60
5000	7.94	9.84	11.87	14.15	16.84	20.21	24.76	31.65	44.77
4000	9.04	10.71	12.56	14.69	17.26	20.53	24.98	31.80	44.84
3000	9.94	11.40	13.08	15.06	17.50	20.66	25.03	31.75	44.72
2000	10.33	11.61	13.13	14.98	17.30	20.35	24.61	31.24	44.12
1900	10.31	11.58	13.09	14.92	17.23	20.26	24.51	31.13	43.97
1800	10.28	11.53	13.02	14.85	17.15	20.17	24.40	31.01	43.81
1700	10.23	11.47	12.95	14.76	17.04	20.05	24.28	30.87	43.63
1600	10.16	11.38	12.85	14.65	16.92	19.92	24.13	30.71	43.44
1500	10.06	11.27	12.73	14.51	16.78	19.76	23.96	30.53	43.22
1400	9.94	11.14	12.58	14.35	16.60	19.58	23.77	30.32	42.98
1300	9.78	10.97	12.40	14.16	16.40	19.36	23.54	30.08	42.71
1200	9.59	10.76	12.18	13.93	16.15	19.10	23.26	29.79	42.39
1100	9.35	10.51	11.91	13.65	15.86	18.79	22.94	29.45	42.03
1000	9.06	10.20	11.59	13.31	15.51	18.42	22.55	29.04	41.59
900	8.70	9.83	11.20	12.91	15.08	17.98	22.08	28.55	41.07
800	8.26	9.37	10.72	12.40	14.55	17.42	21.50	27.94	40.43
700	7.73	8.81	10.13	11.78	13.90	16.74	20.78	27.18	39.63
600	7.07	8.12	9.40	11.00	13.07	15.86	19.85	26.19	38.58
500	6.26	7.24	8.46	10.00	11.99	14.70	18.61	24.86	37.15
400	5.24	6.13	7.24	8.67	10.54	13.12	16.88	22.97	35.09
300	3.94	4.68	5.62	6.85	8.50	10.82	14.28	20.04	31.76
200	2.25	2.73	3.36	4.20	5.39	7.12	9.86	14.67	25.16
100	0	0	0	0	0	0	0	0	0

This article is copyrighted as indicated in the article. Reuse of AIP content is subject to the terms at: http://scitation.aip.org/termsconditions. Downloaded to IP: 130.102.42.98 On: Mon, 24 Nov 2014 09:05:21

$$\frac{\Delta C_p}{\overline{V}T} = \frac{a_2 p_c}{T_c(1-\omega)}(m_\lambda - \omega)^2 \alpha \sim C_p \sim \alpha, \tag{20}$$

where $\overline{V}$ is an average volume in the vicinity of the divergence. The examination of the limiting properties of α, κ, and C_p finally shows that our phenomenological equations have all the requisite properties of pseudocritical divergence along the locus $p_\lambda(T)$.

B. The behavior at high pressures

By increasing pressures, the quantities α and κ decrease in a continuous fashion, however, the heat capacity reaches a minimum as shown in Tables III and IV. The general conditions for the existence of a minimum C_p are given by setting Eq. (1) equal to zero. This minimum determines a line in the plane (p, T), where the quantities α_i, V_i, and p_i are defined accordingly. We have

$$\alpha_i^2 + (\partial\alpha/\partial T)_{p_i} = 0, \quad 1/\alpha_i - T = \text{constant}. \tag{21}$$

Integration of Eq. (21) then gives

$$V_i(T)/V_i(T_0) = 1 + \alpha_{i0}(T - T_0), \tag{22}$$

where, T_0, is a reference temperature and $\alpha_{i0} \equiv \alpha_i(T_0)$. Equation (22) is of a general character emphasizing the small variation of the volume on the locus of the minimum C_p.

Beyond the minimum, the heat capacity increases with the pressure. Proceeding with Eqs. (1) and (10) retaining the dominant term when $\alpha \to 0$, and integrating gives:

$$\frac{\Delta C_p}{\overline{V}T} = \frac{a_2 p_c (m_\lambda - \omega)^2}{T_c(1-\omega)} \frac{\alpha_0^2}{\alpha}. \tag{23}$$

The comparison of Eq. (23) with Eq. (20) gives the general aspect of the behavior of C_p as a function of pressure. When, at low pressures $\Delta C_p \sim (p - p_\lambda)^{-1/2}$, the proportionality is inversed at high pressures with $\Delta C_p \sim (p - p_\lambda)^{1/2}$.

VI. CONCLUSION

The interpolation of the experimental points by a rational function is the result of a choice inspired by the general behavior of the phenomenon. The mathematical method determines, in its reduced form, the unique fraction corresponding to the problem. This unique fraction is consequently the simplest one. The problem is now to know if the *a priori* choice of a rational function is the one most suited to represent the phenomenon. To answer this question, the criteria of simplicity, accuracy, and conformity with thermodynamics were examined. Unfortunately our relatively limited knowledge of liquids does not allow us to go beyond the analysis of the properties in the vicinity of the pseudocritical line. However, finding in this region agreement with the predicted behavior confers to the proposed set of phenomenological equations an unexpected "exactness."

APPENDIX

Figures 8 and 9 give a set of 16 experimental points on the 345.3 K isotherm in the case of *n*-butane. We first decide to ask for a rational fraction $\alpha^n = F(p)$, such that the degree of the denominator is $M = L + 1$. Beginning with $L = 1$ and $M = 2$, the experimental points numbered 3, 7, 11, and 15

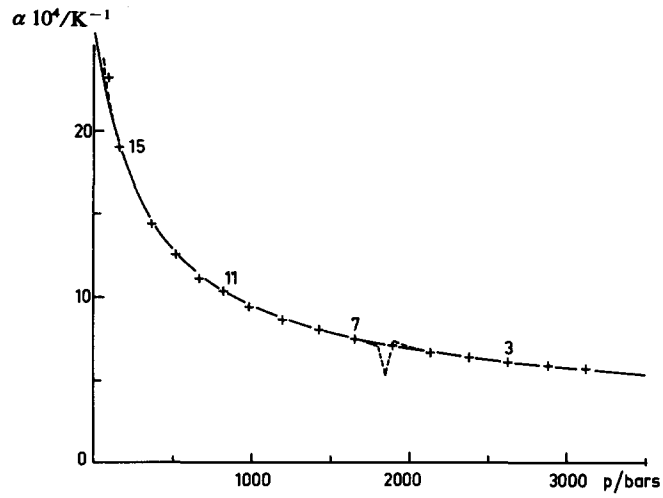

FIG. 8. A set of 16 experimental points on the 345.3 K isotherm in the case of *n*-butane. The full curve gives a very satisfactory fit.

are arbitrarily chosen and give the following result:

$$n = 1, \quad \alpha \times 10^4 = 8.72 \times 10^4 \times \frac{(p + 2.06\times 10^3)}{(p + 2.00\times 10^4)(p + 3.46\times 10^2)}.$$

The full curve in Fig. 8 gives a very satisfactory fit. However we try $n = 2$—with the same points—giving the following result:

$$n = 2, \quad \alpha^2 \times 10^8 = 1.01\times 10^5 \frac{(p - 1854)}{(p - 1858)(p + 120)}.$$

The resulting curve cannot be drawn separately from the former with the exception of a discontinuity occurring around $p = 1856$. Examination of the fraction shows that two factors are mutually balanced to within the limits of the experimental accuracy. The rational fraction for $n = 2$ is consequently overdefined and we may decrease the degrees of the numerator and denominator. For $n = 2$, $L = 0$, $M = 1$, and with the points numbered 7 and 11, we have

$$\alpha^2 \times 10^8 = \frac{862}{1 + 8.72\times 10^{-3} p}.$$

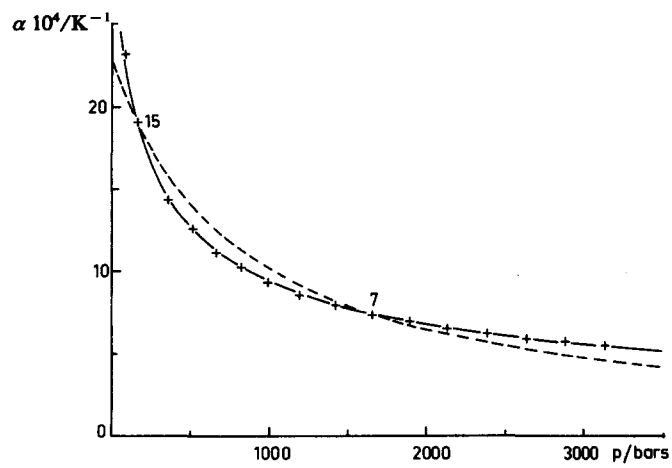

FIG. 9. A set of 16 experimental points on the 345.3 K isotherm in the case of *n*-butane. The full curve gives the resulting fit.

This article is copyrighted as indicated in the article. Reuse of AIP content is subject to the terms at: http://scitation.aip.org/termsconditions. Downloaded to IP: 130.102.42.98 On: Mon, 24 Nov 2014 09:05:21

The full curve (Fig. 9) gives the resulting fit. It is very satisfactory and the fraction cannot be simpler. Trying now a fit for $n = 1, L = 0$ and $M = 1$ with the same points gives the dotted curve in Fig. 9 which evidently does not represent the whole set of experimental points.

[1]P. W. Bridgman, Proc. Am. Acad. Arts Sci. **49**, 3 (1913).
[2]J. C. Petit and L. Ter Minassian, J. Chem. Thermodyn. **6**, 1199 (1974).
[3]L. Ter Minassian, J. C. Petit, Van Kiet Nguyen, and C. Brunaud, J. Chim. Phys. **67**, 265 (1970).
[4]L. Ter Minassian and P. Pruzan, J. Chem. Phys. **75**, 3064 (1981).
[5]L. Ter Minassian and F. Milliou, J. Phys. E **16**, 450 (1983).
[6]H. Werner, Lectures Notes Math. **76**, 257 (1979).
[7]L. Ter Minassian and P. Pruzan, J. Chem. Thermodyn. **9**, 375 (1977).
[8]J. A. Baker Jr. and P. R. Graves-Morris, *Encyclopedia of Mathematics* (Addison–Wesley, Reading, Mass., 1981), Vol. 16.
[9]A. Denis, (to be published).
[10]P. Claverie and A. Denis, SIAM J. Math. Anal. (submitted).
[11]*International Thermodynamic Tables of the Fluid State*, edited by Angus, Armstrong, de Reuck (Pergamon, London, 1976), Vol. 3.
[12]W. H. Haynes and R. D. Goodwin, NBS Monogr. **169**, 1982.
[13]L. L. Pitaevskaya and A. V. Bilevitch, Sov. Phys. Dokl. **16**, 1, 33 (1971).
[14]W. L. Jorgensen, J. Am. Chem. Soc. **103**, 4721 (1981).
[15]V. C. Altunin and O. G. Gadetskii, Therm. Eng. (USSR) **18**, 120 (1971).
[16]A. Compagner, Physical **72**, 115 (1974).
[17]R. R. Speedy, J. Phys. Chem. **86**, 3002 (1982).
[18]P. W. Bridgman, Proc. Am. Acad. Arts Sci. **77**, 129 (1949).
[19]J. J. Nicolas, K. E. Gubbins, W. B. Streett, and D. J. Tildesley, Mol. Phys. **37**, 1429 (1979).
[20]W. B. Streett, Physica **76**, 59 (1974).
[21]H. B. Dwight, *Tables of Integrals* (Macmillan, New York, 1957).

This article is copyrighted as indicated in the article. Reuse of AIP content is subject to the terms at: http://scitation.aip.org/termsconditions. Downloaded to IP: 130.102.42.98 On: Mon, 24 Nov 2014 09:05:21